Available online at www.sciencedirect.com
ScienceDirect
Journal of Environmental Sciences 2010, 22(1) 91–97
JOURNAL OF ENVIRONMENTAL SCIENCES
ISSN 1001-0742
CN 11-2629/X
www.jesc.ac.cn

Preparation of activated carbon from cattail and its application for dyes removal

Qianqian Shi[1], Jian Zhang[1,*], Chenglu Zhang[1], Cong Li[1], Bo Zhang[1], Weiwei Hu[2], Jingtao Xu[1], Ran Zhao[1]

1. School of Environmental Science and Engineering, Shandong University, Jinan 250100, China. E-mail: shuipingdingding@gmail.com
2. State Key Joint Laboratory of Environmental Simulation and Pollution Control, College of Environmental Sciences and Engineering, Peking University, Beijing 100871, China

Received 25 February 2009; revised 14 August 2009; accepted 28 August 2009

Abstract

Activated carbon was prepared from cattail by H_3PO_4 activation. The effects influencing the surface area of the resulting activated carbon followed the sequence of activated temperature > activated time > impregnation ratio > impregnation time. The optimum condition was found at an impregnation ratio of 2.5, an impregnation time of 9 hr, an activated temperature of 500°C, and an activated time of 80 min. The Brunauer-Emmett-Teller surface area and average pore size of the activated carbon were 1279 m^2/g and 5.585 nm, respectively. A heterogeneous structure in terms of both size and shape was highly developed and widely distributed on the carbon surface. Some groups containing oxygen and phosphorus were formed, and the carboxyl group was the major oxygen-containing functional group. An isotherm equilibrium study was carried out to investigate the adsorption capacity of the activated carbon. The data fit the Langmuir isotherm equation, with maximum monolayer adsorption capacities of 192.30 mg/g for Neutral Red and 196.08 mg/g for Malachite Green. Dye-exhausted carbon could be regenerated effectively by thermal treatment. The results indicated that cattail-derived activated carbon was a promising adsorbent for the removal of cationic dyes from aqueous solutions.

Key words: cattail; activated carbon; H_3PO_4 activation; dyes removal; regeneration

DOI: 10.1016/S1001-0742(09)60079-6

Introduction

Cattail is one of the most common aquatic plants, and it can be found worldwide in wetlands, fens, margins of ponds and lakes, roadside ditches, irrigation canals, and backwater areas of rivers and streams (Kim et al., 2003). It is a very recognizable aquatic wetland plant that can provide excellent cover and nesting habitat for certain wildlife. Cattail can utilize solar energy effectively and grow rapidly. Its rapid growth produces a large amount of biomass, which can become a potential pollution resource to the environment (Hu and Yu, 2006). This motivates the investigation of producing value-added products, such as activated carbon, from this abundant material.

Activated carbon is a well-known material used in both gas and liquid phases, including medicinal use, gas storage, pollutant and odor removal, gas separation, and catalysis (Nabais et al., 2008). However, commercially available activated carbons are still considered expensive materials for many countries due to the use of non-renewable and relatively expensive starting materials such as coal (Martin et al., 2003). Practically any carbonaceous material, natural or synthetic, rich in carbon and low in ash, is theoretically feasible for activated carbon production (Attia et al., 2008). Therefore, in recent years, this has prompted a growing interest in the research on the production of activated carbons from cheaper and renewable precursors, which are mainly industrial and agricultural byproducts, such as rice hull (Guo and Rockstraw, 2007), olive cake (Aljundi and Jarrah, 2008), corncob (Tseng et al., 2006), apricot stone (Karagozoglu et al., 2007), date stone (Bouchelta et al., 2008), coconut husk (Tan et al., 2008), rattan sawdust (Hameed et al., 2008), and bagasse bottom ash (Aworn et al., 2008). However, there are only a few reports on the preparation of cattail-derived activated carbon.

The manufacture of activated carbons generally involves two steps: pyrolysis and physical and/or chemical activation. Compared with physical activation, chemical activation has a lower temperature and a higher carbon product yield (Uğurlu et al., 2008). Chemical activation consists of carbonization in the presence of a dehydrating chemical agent (e.g., $ZnCl_2$, H_3PO_4, and H_2SO_4). These chemical agents enhance carbonization, thus resulting in the development of a desired pore structure. From both economic and environmental perspectives, H_3PO_4 is the preferred chemical agent because it is recoverable (Guo and Rockstraw, 2006), and the activation temperature

* Corresponding author. E-mail: zhangjian00@sdu.edu.cn

involved is relatively low (around 400–500°C).

The principal objective of this study is to prepare an activated carbon from cattail by H_3PO_4 activation and measure its dye adsorption properties. In order to optimize the experimental procedure, orthogonal array design (OAD) was employed. The theory and methodology of OAD as a chemometric method for the optimization of analytical procedures has been described in detail elsewhere (Sobhi et al., 2008; Yamini et al., 2008). OAD procedure with OA_9 (3^4) matrix was applied to study the effect of experimental factors on the carbon surface area. The results of OAD experiment were then treated by range analysis. The sample under optimum condition was analyzed for a detailed study of its carbon characteristics, dye adsorption, and thermal regeneration. Two cationic dyes, Neutral Red and Malachite Green, were selected as absorbates in the adsorption and regeneration experiments.

1 Materials and methods

1.1 Raw material

Cattail used in this study was obtained from a local wetland near Jinan, China. All reagents were analytical grade.

1.2 Preparation of activated carbon

Cattail was washed, dried, ground in a laboratory mill, and then impregnated with a 40 wt.% H_3PO_4 solution at a certain ratio. The resulting wet mass was placed in a muffle furnace and heated for several minutes with the final activated temperatures. It was cooled down afterwards to room temperature. The carbonized material produced was washed with deionized water until its filtrate reached neutral pH and then dried at 120°C for 2 hr.

1.3 Orthogonal experiment

OA_9 (3^4) matrix was employed to study the effect of four factors influencing the carbon surface area: impregnation ratio, impregnation time, activated temperature, and activated time. Emphasis was placed on the main effect of the four factors; thus, the possible interactions between them were not in the matrix. The factors and levels of orthogonal experiment are presented in Table 1.

1.4 Characterization of activated carbon

The textural properties of activated carbon were determined by N_2 adsorption (at –196°C) using QUADRASORB SI automated surface area and pore size analyzer (Quantachrome Corporation, USA). The surface area and pore size distribution were estimated following the Brunauer-Emmett-Teller (BET) method and Density Functional Theory (DFT) method, respectively. The total volume and average pore size were measured using Quadrawin software. The micropore volume and external surface area were calculated by the *t*-plot method.

Table 1 Factors and levels of the orthogonal experiment

Level	Impregnation ratio (m_H:m_C)	Impregnation time (hr)	Activated temperature (°C)	Activated time (min)
1	2.2	6	400	40
2	2.5	9	450	60
3	2.8	12	500	80

m_H: amount of phosphoric acid; m_C: amount of cattail.

The surface morphology of carbon was observed by scanning electron microscopy (SEM) (Hitachi S-520, Japan). The sample was gold coated prior to SEM observation. The surface chemistry characterization of the sample was performed using Fourier Transform Infrared Spectroscopy (FT-IR) and Boehm titration. The infrared spectrum of carbon was recorded at room temperature by an Avatar 370 spectrometer (Nicolet Instrument Corporation, USA) using the KBr disc method. Boehm titration was employed to determine the acidic surface groups of carbon qualitatively (Boehm, 1966).

1.5 Adsorption experiments

Two cationic dyes, Neutral Red (NR, $C_{15}H_{16}N_4HCl$, λ_{max} = 530 nm) and Malachite Green (MG, $C_{23}H_{25}N_2Cl$, λ_{max} = 618 nm), were used in the experiments. For each experiment, 100 mg of activated carbon was added to a 100-mL dye solution, with an initial concentration ranging from 80 to 200 mg/L. Afterwards, the mixture was shaken for 250 min at 10, 26, and 45°C. The residual concentration was determined by measuring its absorbance in a UV-Visible spectrophotometer (UV-754, Shanghai, China) at the maximum wavelength of the dye. The amount of dye adsorbed was calculated from the following mass balance equation (Eq. (1)):

$$q_e = \frac{(C_0 - C_1)\,V}{m} \tag{1}$$

where, C_0 and C_1 are the initial and final dye concentrations, respectively; V is the volume of solution; and m is the mass of carbon.

1.6 Thermal regeneration of spent activated carbon

In the experiment, 300 mg of carbon was added to a 300-mL dye solution (200 mg/L), and the suspension was mechanically shaken for 250 min at 26°C. The solution was then filtered out, and the amount of dye adsorbed was calculated. The spent activated carbon was loaded into the furnace, heated at 300°C for 30 min, and then allowed to cool down at room temperature. Subsequently, the adsorption experiment was carried out again to evaluate the regeneration efficiency (R) of carbon, which was calculated according to the following expression (Eq. (2)):

$$R = \frac{M_{rc}}{M_{vc}} \tag{2}$$

where, M_{rc} and M_{vc} are amounts adsorbed on regenerated and virgin carbon, respectively.

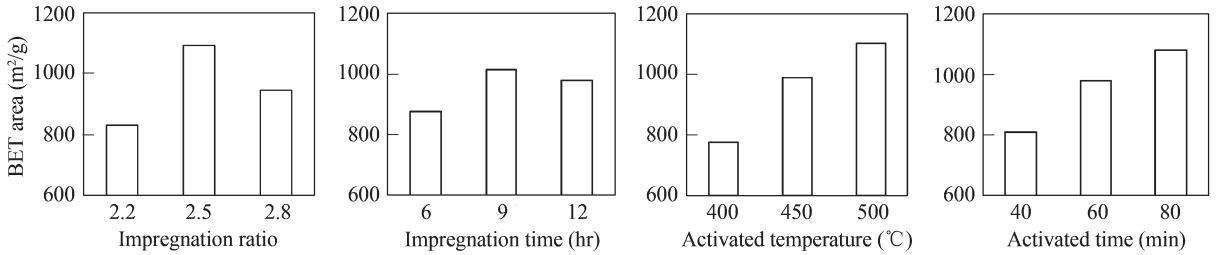

Fig. 1 Effects of factors on the BET surface area of activated carbon.

2 Results and discussion

2.1 Range analysis

The results of designing the orthogonal experiment are shown in Table 2. Under the range analysis, the average of BET surface areas for each factor at different levels (K_1, K_2, and K_3) and the range R are given in Table 2.

The impregnation ratio (A), impregnation time (B), activated temperature (C), and activated time (D) all affected the BET surface area. As shown in Fig. 1, the mean values (K_1, K_2 and K_3) reveal how the BET surface area will change when the level of that factor is changed as well. As shown in Table 2, with decrease sequence of R, the order of factors influencing BET surface area was C > D > A > B. The results of K were K_2 (A) > K_3 (A) > K_1 (A), K_2 (B) > K_3 (B) > K_1 (B), K_3 (C) > K_2 (C) > K_1 (C), and K_3 (D) > K_2 (D) > K_1 (D). Therefore, the best combination was $A_2B_2C_3D_3$, that is, the optimum condition had an impregnation ratio 2.5, impregnation time 9 hr, activated temperature 500°C, and activated time 80 min.

2.2 Additional experiment

The optimum condition was not included in the experimental combinations. Therefore, an additional experiment under this condition was carried out to verify the combination $A_2B_2C_3D_3$ with the largest BET surface area. The result of the BET surface area in the additional experiment was 1279 m^2/g, which was larger than any value of the BET surface area above, confirming that the optimum condition was suitable. The result reported here may also be compared with that of commercially available carbons, which typically have a surface area in the range 400–1500 m^2/g (Williams and Reed, 2003). The activated carbon obtained under the optimum condition (named as AC-1) was then used for carbon characteristics, dye adsorption, and thermal regeneration.

2.3 Surface area and pore size distribution

N_2 adsorption is considered the standard procedure for the characterization of the porosity texture of carbonaceous adsorbents. The isotherm can provide information on the porous structure of the adsorbent, heat of adsorption, characteristics of physics and chemistry, and so on (Önal, 2006). Figure 2 shows the N_2 adsorption/desorption isotherm (–196°C) of AC-1, which is classified as a type IV according to International Union of Pure and Applied Chemistry. The isotherm indicates the micro-mesoporous structure of the carbon. The initial part of the isotherm follows the same path as the corresponding type II isotherm, and thus resulting to the monolayer-multilayer adsorption on the mesopore walls (Ryu et al., 1999).

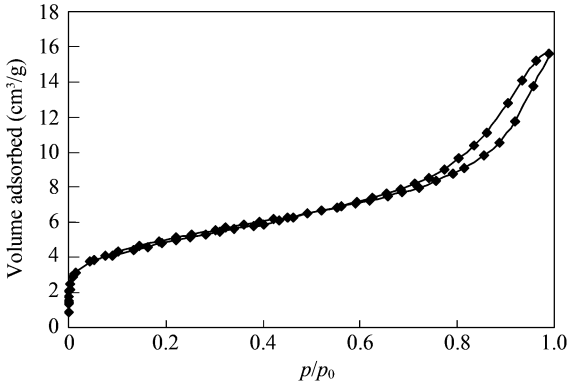

Fig. 2 Adsorption/desorption isotherm of nitrogen at –196°C for AC-1.

The adsorption measurement provides a useful "fingerprint" of the microstructure, and it is essential if the carbon is utilized as an adsorbent or catalyst support. The pore size distribution seems to provide especially useful information on porous solids (Seaton et al., 1989). Figure 3 shows the pore size distribution of AC-1, the results of which and the BET surface area are presented in Table 3. It is observed that the activated carbon prepared from cattail has a high surface area, which is primarily attributed to the mesopores and macropores as the percent contribution of micropores is only 13.6% of the BET surface area. The total pore volume was as high as 1.786 cm^3/g for AC-1, which could be compared with that of commercially activated carbons, that is, 0.60 and 0.52 cm^3/g for carbons BPL and PCB produced by Calgon Carbon Co., Pittsburgh, USA, respectively (Ioannidou and Zabaniotou, 2007). The average pore size of 5.585 nm was also obtained. These illustrate the notion that cattail is a suitable precursor for the preparation of meso-activated carbon by H_3PO_4 activation.

2.4 SEM analysis of microstructure

The microstructure of AC-1 is shown in Fig. 4. The scanning electron micrograph of AC-1 showed an irregular and heterogeneous surface morphology with a well-developed porous structure. Pores of different sizes shapes could be observed. The external surface of the activated carbon was full of cavities and quite irregular. The development of the pore system in carbon depends on the structure of the starting material and the activated

Table 2 Design and results of the orthogonal experiment

Number	Impregnation ratio (m_H:m_C)	Impregnation time (hr)	Activated temperature(°C)	Activated time (min)	BET surface area (m^2/g)
1	1	1	1	1	419
2	1	2	2	2	948
3	1	3	3	3	1121
4	2	1	3	2	1182
5	2	2	1	3	1093
6	2	3	2	1	1003
7	3	1	2	3	1023
8	3	2	3	1	1000
9	3	3	1	2	812
K_1	829.3	874.7	774.7	807.3	
K_2	1092.7	1013.7	991.3	980.7	
K_3	945	978.7	1101	1079	
R	263.4	139	326.3	271.7	

m_H: amount of phosphoric acid; m_C: amount of cattail. K (K_1, K_2, K_3) is the average of BET surface areas for each factor at different levels.

Table 3 Surface area and porosity of AC-1

S_{BET} (m^2/g)	S_{ext} (m^2/g)	S_{ext} (%)	S_{mic} (m^2/g)	S_{mic} (%)	V_t (cm^3/g)	V_{mic} (cm^3/g)	V_{mic} (%)	D_p (nm)
1279	1105	86.4	174	13.6	1.786	0.088	4.93	5.585

S_{BET}: BET surface area; S_{ext}: external surface area; S_{mic}: micropore surface area; V_t: total pore volume; V_{mic}: micropore volume; D_p: average pore size.

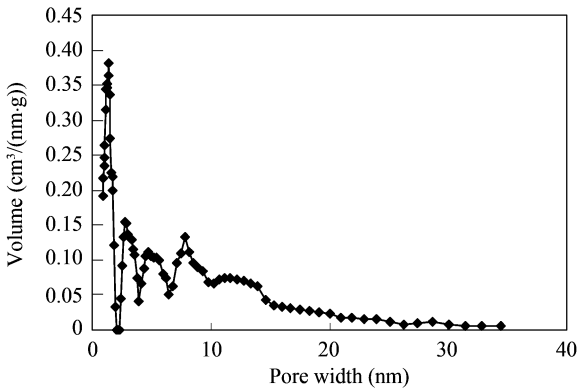

Fig. 3 Pore size distribution of AC-1.

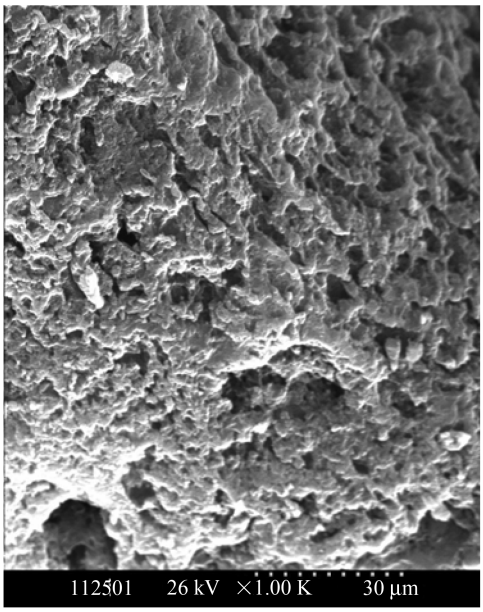

Fig. 4 Scanning electron micrograph of AC-1.

process. The cavities resulted from the evaporation of the chemical reagent (H_3PO_4) during carbonization, leaving the space previously occupied by the reagent (El-Hendawy et al., 2008).

2.5 Fourier transform infrared spectroscopy (FT-IR) results

In this study, FT-IR was used to obtain information on the chemical structure and functional groups of the prepared activated carbon (Fig. 5). A broad band located around 3400 cm^{-1} is typically attributed to the hydroxyl groups or adsorbed water. The band around 1700 cm^{-1} is usually caused by the stretching vibration of C═O in ketones, aldehydes, lactones, and carboxyl groups, while the band around 1600 cm^{-1} is ascribed to the aromatic ring or C═C stretching vibration. This indicates the formation of carbonyl-containing groups and the aromatization of the precursor (Guo and Rockstraw, 2007). The band around 1220 cm^{-1} is typically attributed to the C–O band. In H_3PO_4 activation, the reagent (H_3PO_4) promotes depolymerization, dehydration, and redistribution of constituent biopolymers, inducing important changes in the pyrolytic decomposition of the lignocellulosic materials and thus favoring the conversion of aliphatic to aromatic compounds at low temperatures (Jagtoyen and Derbyshire, 1993). For the FT-IR spectrum of carbon prepared by H_3PO_4 activation, the band in the region of 1300–900 cm^{-1} could be caused by the phosphorus-containing groups. The peak around 1220–1180 cm^{-1} could be attributed to the stretching of P═O bond in a phosphate ester, O–C bond in P–O–C linkage, or P═OOH bond. This indicates the presence of phosphorus-containing groups in the carbon (Puziy et al., 2002).

2.6 Boehm titration

Boehm titration is one of the most widely used methods to quantify acidic groups with different strengths on

activated carbons. It is initially used for the differentiation of oxygen-containing groups, including carboxyl, lactone, phenol, and carbonyl groups. On the surface of AC-1, carboxyl, lactone, and carbonyl groups were detected, the concentrations of which were 1.695, 0.028, and 0.181 meq/g, respectively. The concentration of carboxyl group was significantly higher compared with the other two groups, indicating that carboxyl group was more prevalent on the surface of AC-1.

2.7 Adsorption isotherms of AC-1 for the dyes

The produced activated carbon (AC-1) was tested for its adsorption capacity for NR and MG. The amount of dye adsorbed can be determined as a function of the concentration at a constant temperature, which can be explained by adsorption isotherms. In this study, analysis of the adsorption isotherms was carried out by applying the linear Langmuir equation (Eq. (3)):

$$\frac{C_e}{q_e} = \frac{1}{Q_m K_L} + \frac{C_e}{Q_m} \tag{3}$$

and the Freundlich equation (Thinakaran et al., 2008),

$$\log q_e = \log K_F + \frac{1}{n}\log C_e \tag{4}$$

where, C_e (mg/L) is the concentration of the dye solution at equilibrium; q_e (mg/g) is the amount of dye adsorbed per unit weight of activated carbon at equilibrium; K_L (L/mg) is a Langmuir constant related to the free energy of adsorption; and Q_m (mg/g) is the maximum adsorption capacity. K_F is a Freundlich constant indicating the relative adsorption capacity of the carbon, and $1/n$ is the adsorption intensity.

The Langmuir and Freundlich plots for the system studied are presented in Fig. 6, while the isotherm constants and correlation coefficients are given in Table 4. The Langmuir and Freundlich isotherms of NR and MG were found to be linear over the whole concentration range studies, and the R^2 values showed that the Langmuir model fit better than the Freundlich model. The values of Q_m increased as the temperature rose, thereby confirming that the processes were both endothermic. At 45°C, the maximum adsorption capacities were determined as 192.30 and 196.08 mg/g for NR and MG, respectively. This can be compared with the data from the literature. For instance, Başar (2006) reported that the maximum adsorption capacity at 50°C was determined as 163.93 mg/g for MG on apricot-derived activated carbon. Yuan et al. (2007) found that the maximum adsorption capacity at 20°C was approximately 113 mg/g for NR on a microporous carbon. The values of $1/n$ in Table 4 were found to be between 0 and 1, indicating a favorable adsorption of NR and MG on AC-1.

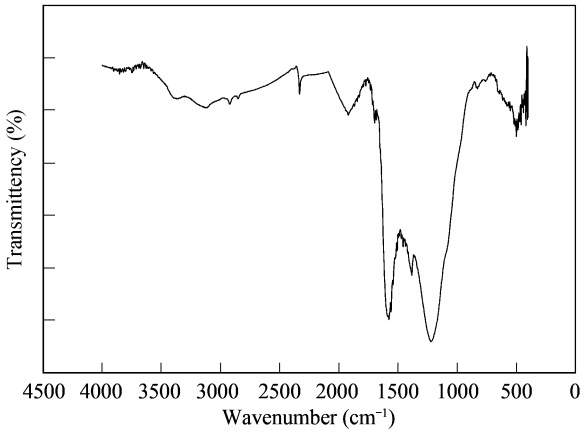

Fig. 5 FT-IR spectrum of AC-1.

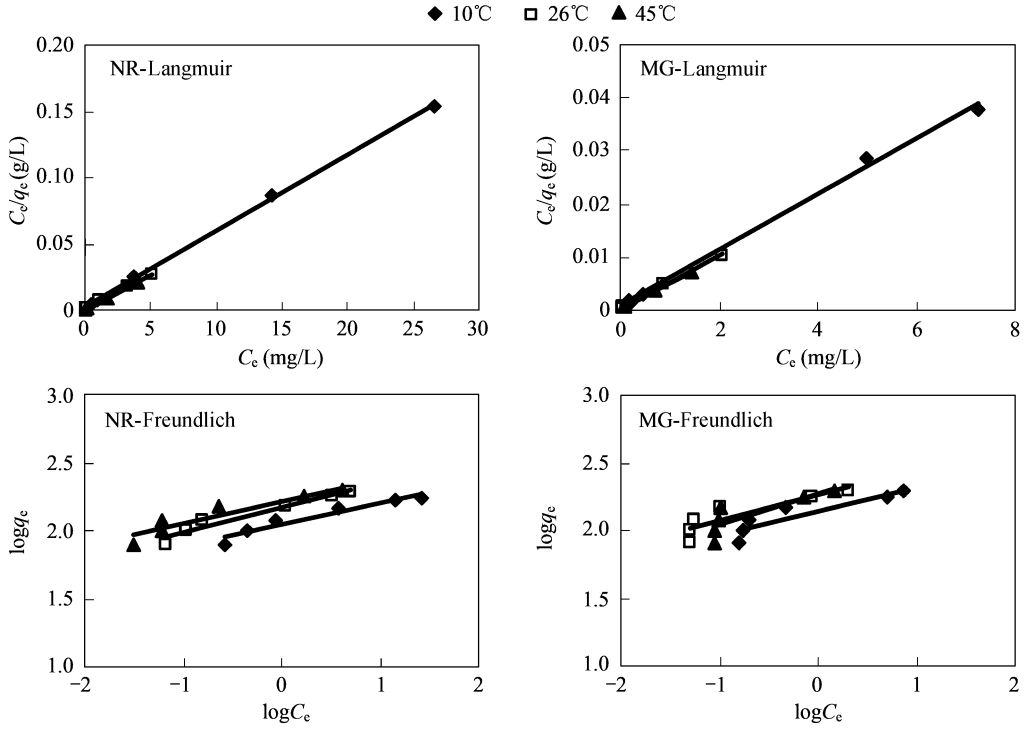

Fig. 6 Isotherm plots for the adsorption of Neutral Red (NR) and Malachite Green (MG) onto AC-1.

Table 4 Isotherm constants and correlation coefficients for the removal of NR and MG by AC-1

Dye	Temperature (°C)	Langmuir			Freundlich		
		Q_m (mg/g)	K_L (L/mg)	R^2	K_F ((mg/g)(L/mg)$^{1/n}$)	$1/n$	R^2
Neutral Red	10	181.81	1.30	0.9995	113.58	0.16	0.9261
	26	188.68	2.40	0.9956	128.32	0.15	0.9442
	45	192.30	3.93	0.9988	136.83	0.16	0.8819
Malachite Green	10	192.30	1.86	0.9971	121.90	0.19	0.7967
	26	192.30	3.06	0.9987	135.96	0.16	0.7679
	45	196.08	5.67	0.9957	149.97	0.15	0.6818

2.8 Regeneration of AC-1

To be a promising adsorbent, AC-1 should be readily regenerated. Experimental results showed that the adsorption capacities of the regenerated AC-1 were determined as 161.68 and 157.64 mg/g for NR and MG, and the regeneration efficiencies were 82.96% and 79.64%, respectively. This demonstrates the effectiveness of thermal treatment in the regeneration of dye-exhausted AC-1, and it is expected that this method can be applied to regenerate AC-1 exhausted with other organic pollutants.

3 Conclusions

In the study, an activated carbon with high surface area was prepared from a commonly available hydrophyte-cattail by H_3PO_4 activation. Orthogonal analysis was used to investigate the factors influencing the surface area, the sequence of which was activated temperature > activated time > impregnation ratio > impregnation time. The best condition for the carbon production was as follows: impregnation ratio = 2.5, impregnation time = 9 hr, activated temperature = 500°C, and activated time = 80 min. At the optimum condition, the activated carbon obtained was essentially mesoporous with a BET surface area of 1279 m^2/g and average pore size of 5.585 nm. The SEM showed a heterogeneous surface with a well-developed porous structure. FT-IR proved the presence of different oxygen-containing and phosphorus-containing groups. Carboxyl, lactone, and carbonyl groups were measured by Boehm titration, with the carboxyl group being the major oxygen functional group on the carbon surface. The activated carbon could effectively remove NR and MG from aqueous solutions. The equilibrium data followed the Langmuir model, showing the maximum monolayer adsorption capacities of 192.30 mg/g for NR and 196.08 mg/g for MG. Thermal treatment effectively regenerated the adsorption capacities of carbon, with the regeneration efficiencies being high. In conclusion, cattail is a potential and low-cost natural material for the preparation of activated carbon.

Acknowledgments

The work was supported by the National Key Technology R&D Program for the 11th Five-year Plan of China (No. 2006BAC10B03), the National Natural Science Foundation of China-Japan Science and Technology Agency (NSFC-JST) Strategic Joint Research Project (No. 50721140017), and the National Natural Science Foundation of China (No. 50508019).

References

Aljundi I H, Jarrah N, 2008. A study of characteristics of activated carbon produced from Jordanian olive cake. *Journal of Analytical and Applied Pyrolysis*, 81(1): 33–36.

Attia A A, Girgis B S, Fathy N A, 2008. Removal of methylene blue by carbons derived from peach stones by H_3PO_4 activation: batch and column studies. *Dyes and Pigments*, 76(1): 282–289.

Aworn A, Thiravetyan P, Nakbanpote W, 2008. Preparation and characteristics of agricultural waste activated carbon by physical activation having micro- and mesopores. *Journal of Analytical and Applied Pyrolysis*, 82(2): 279–285.

Başar C A, 2006. Applicability of the various adsorption models of three dyes adsorption onto activated carbon prepared waste apricot. *Journal of Hazardous Materials*, 135(1-3): 232–241.

Boehm H P, 1966. Chemical identification of surface groups. *Advances in Catalysis*, 16: 179–274.

Bouchelta C, Medjram M S, Bertrand O, Bellat J P, 2008. Preparation and characterization of activated carbon from date stones by physical activation with steam. *Journal of Analytical and Applied Pyrolysis*, 82(1): 70–77.

El-Hendawy A N A, Alexander A J, Andrews R J, Forrest G, 2008. Effects of activation schemes on porous, surface and thermal properties of activated carbons prepared from cotton stalks. *Journal of Analytical and Applied Pyrolysis*, 82(2): 272–278.

Guo Y, Rockstraw D A, 2006. Physical and chemical properties of carbons synthesized from xylan, cellulose, and Kraft lignin by H_3PO_4 activation. *Carbon*, 44(8): 1464–1475.

Guo Y, Rockstraw D A, 2007. Activated carbons prepared from rice hull by one-step phosphoric acid activation. *Microporous and Mesoporous Materials*, 100(1-3): 12–19.

Hameed B H, Chin L H, Rengaraj S, 2008. Adsorption of 4-chlorophenol onto activated carbon prepared from rattan sawdust. *Desalination*, 225(1-3): 185–198.

Hu Z H, Yu H Q, 2006. Anaerobic digestion of cattail by rumen cultures. *Waste Management*, 26(11): 1222–1228.

Ioannidou O, Zabaniotou A, 2007. Agricultural residues as precursors for activated carbon production – a review. *Renewable and Sustainable Energy Reviews*, 11(9): 1966–2005.

Jagtoyen M, Derbyshire F, 1993. Some considerations of the origins of porosity in carbons from chemically activated wood. *Carbon*, 31: 1185–1192.

Karagozoglu B, Tasdemir M, Demirbas E, Kobya M, 2007. The adsorption of basic dye (Astrazon Blue FGRL) from aqueous solutions onto sepiolite, fly ash and apricot shell activated carbon: kinetic and equilibrium studies. *Journal of Hazardous Materials*, 147(1-2): 297–306.

Kim C, Shin H, Choi H K, 2003. A phenetic analysis of Typha in Korea and far east Russia. *Aquatic Botany*, 75(1): 33–43.

Martin M J, Artola A, Balaguer M D, Rigola M, 2003. Activated carbons developed from surplus sewage sludge for the removal of dyes from dilute aqueous solutions. *Chemical Engineering Journal*, 94(3): 231–239.

Nabais J V, Carrott P, Carrott M M L R, Luz V, Ortiz A L, 2008. Influence of preparation conditions in the textural and chemical properties of activated carbons from a novel biomass precursor: the coffee endocarp. *Bioresource Technology*, 99(15): 7224–7231.

Önal Y, 2006. Kinetics of adsorption of dyes from aqueous solution using activated carbon prepared from waste apricot. *Journal of Hazardous Materials*, 137(3): 1719–1728.

Puziy A M, Poddubnaya O I, Martínez-Alonso A, Suárez-García F, Tascón J M D, 2002. Synthetic carbons activated with phosphoric acid: I. Surface chemistry and ion binding properties. *Carbon*, 40(9): 1493–1505.

Ryu Z, Zheng J, Wang M, Zhang B, 1999. Characterization of pore size distributions on carbonaceous adsorbents by DFT. *Carbon*, 37(8): 1257–1264.

Seaton N A, Walton J P R B, Quirke N, 1989. A new analysis method for the determination of the pore size distribution of porous carbons from nitrogen adsorption measurements. *Carbon*, 27(6): 853–861.

Sobhi H R, Yamini Y, Esrafili A, Abadi R H H B, 2008. Suitable conditions for liquid-phase microextraction using solidification of a floating drop for extraction of fat-soluble vitamins established using an orthogonal array experimental design. *Journal of Chromatography A*, 1196-1197(1-2): 28–32.

Tan I A W, Ahmad A L, Hameed B H, 2008. Adsorption of basic dye on high-surface-area activated carbon prepared from coconut husk: equilibrium, kinetic and thermodynamic studies. *Journal of Hazardous Materials*, 154(1-3): 337–346.

Thinakaran N, Panneerselvam P, Baskaralingam P, Elango D, Sivanesan S, 2008. Equilibrium and kinetic studies on the removal of Acid Red 114 from aqueous solutions using activated carbons prepared from seed shells. *Journal of Hazardous Materials*, 158(1): 142–150.

Tseng R L, Tseng S K, Wu F C, 2006. Preparation of high surface-area carbons from corncob with KOH etching plus CO_2 gasification for the adsorption of dyes and phenols from water. *Colloids and Surfaces A: Physicochemical and Engineering Aspects*, 279(1-3): 69–78.

Uğurlu M, Gürses A, Açıkyıldız M, 2008. Comparison of textile dyeing effluent adsorption on commercial activated carbon and activated carbon prepared from olive stone by $ZnCl_2$ activation. *Microporous and Mesoporous Materials*, 111(1-3): 228–235.

Williams P T, Reed A R, 2003. Pre-formed activated carbon matting derived from the pyrolysis of biomass natural fiber textile waste. *Journal of Analytical and Applied Pyrolysis*, 70(2): 563–577.

Yamini Y, Saleh A, Khajeh M, 2008. Orthogonal array design for the optimization of supercritical carbon dioxide extraction of platinum(IV) and rhenium(VII) from a solid matrix using cyanex 301. *Separation and Purification Technology*, 61(1): 109–114.

Yuan X, Zhuo S P, Xing W, Cui H Y, Dai X D, Liu X M et al., 2007. Aqueous dye adsorption on ordered mesoporous carbons. *Journal of Colloid and Interface Science*, 310(1): 83–89.